# Supporting Information for:

# Ligand exchange based molecular doping in 2D hybrid molecule-nanoparticle arrays: length determines exchange efficiency and conductance change

Cliff E. McCold[1‡], Qiang Fu[2‡], Sahar Hihath[1], Ji-Min Han[3], Yaeir Halfon[4], Roland Faller[4], Klaus van Benthem[1], Ling Zang[3], and Joshua Hihath[2,*].

[1]Materials Science and Engineering, UC Davis. [2]Electrical and Computer Engineering, UC Davis. [3]Materials Science and Engineering, University of Utah. [4]Chemical Engineering, UC Davis

Contents



## 1. Au Nanoparticle Synthesis and phase transfer

Traditional aqueous synthesis of citrate-capped Au NPs was performed using the methods of Tsutsui, et al.[1] Briefly, hydrogen tetrachloroaurate trihydrate was reduced by citrate dehydrate and tannic acid. Two solutions are used. The first solution is 1ml of 1% (weight) HAuCl3*3H20 is added to 79 mL distilled water. The second solution is 4 mL of 1% (weight) trisodium citrate dehydrate, 0.08 mL tannic acid, and 16 mL distilled water. Both solutions are heated to 60 °C and then mixed with stirring. Heating is increased to boiling for 10 minutes, then solution is cooled in ice water for 1 h. One 30 min spin cycle in an Espresso microcentrifuge at 12k RCF separates the product from the reactant and the product is resuspended in water.

To perform phase transfer, aqueous NP solution is spun at 12k RCF for 20 min and decanted. The product is resuspended in 20 mM alkanethiol in 100% ethanol and shaken. After 18 h, particles are solid on the eppendorf bottom and the clear ethanol is pipetted out and the eppendorf is dried under nitrogen flow. The dried particles are resuspended in 100% chloroform, sonicated briefly, and used immediately.

## 2. PTCDI Synthesis

PTCDI was synthesized according to published methods.[2]

3. Transmission electron microscopy (TEM)

TEM samples of nanoparticles were prepared by microcontact printing method, which is described in the manuscript, on PELCO silicon nitride support films by Ted Pella. TEM imaging of the nanoparticle array was performed at 200 keV at the University of California Davis with a JEOL-JEM 2500SE instrument.

4. Image analysis and molecular lengths

For Figure 2.A, nanoparticle size analysis was performed in ImageJ[3] using contrast thresholding and the built-in Analyze Particles function. Diameters were determined as the diameter of a circle with the same area as the particle area in the analyzed images. Particle separations were measured manually on hundreds of gaps in images for each molecular sample. Molecular lengths were calculated using ACD/Labs Chemsketch[4].

5. Temperature Dependence of Conductance

Charge transport in these nanoparticle arrays is expected to be by thermally activated hopping from nanoparticle site to nanoparticle site. Temperature dependent measurements from 23 – 50 °C were performed on PTCDI chips exchanged from C16. Errors bars are standard deviation of three measurements. Results are consistent with a thermally activated hopping conductance mechanism. The slope of the corresponding $Ln(G/G_{RT})$ vs. 1/T plot allows us to calculate an activation energy of 26.6+/-0.7 meV for PTCDI-state arrays.

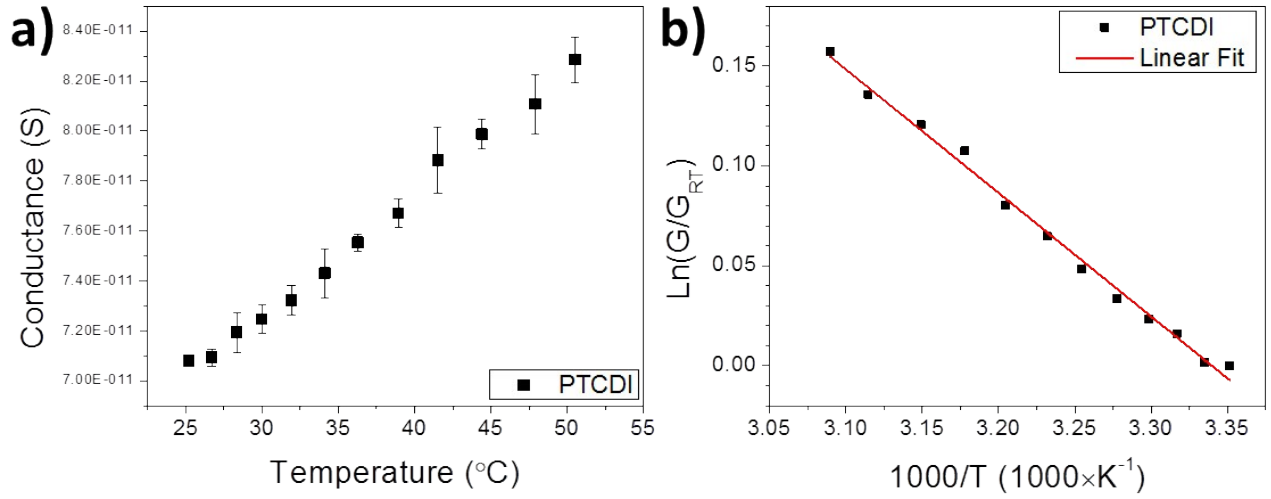


**Figure S1. Temperature dependence and Arrhenius plot for PTCDI state NP arrays.** A) Average conductance as a function of temperature for three measurements. Error bars are standard deviation of three measurements. B) Arrhenius-type plot for the conductance data shown in (a). $G_{RT}$ is the conductance at room temperature. An activation energy of 26.6±0.7 meV is found from the slope.

Details of extracting the temperature dependence into manuscript equation 1 from n and μ. Traditionally $\sigma = nq\mu$ and exponential temperature dependence are in N and μ, and the tunneling probability is in μ. To

allow us to express these dependencies clearly in the conductance equation 1 in manuscript, we define $N_0 = \frac{n}{exp\left(-E_A/k_BT\right)}$ and $\mu_0 = \frac{\mu}{exp\left(-E_A/k_BT\right)exp(-\beta s)}$.

6. Monte Carlo Simulation

A script for simulating hopping-based charge transport in 2-D arrays was written and executed in Matlab (Mathworks, Natick, MA). Hexagonal grids (with each non-edge node having 6 nearest neighbors) were generated where the separations between each node were selected from a Gaussian distribution corresponding to the separations measured from TEM. Grids contained 588 nodes in a rectangular geometry with a 3:1 width:length ratio, which matched the experimental device geometry (Fig. 1c). The simulation was run by having a charge carrier start at one side of the rectangular grid (at the source electrode) on a random edge node. For alkane molecules, the probability of successfully hopping from one node (particle) to another node (particle) was determined by standard Metropolis Monte Carlo according to $exp(-\beta s)exp(p \cdot h\, V_{bias})exp\left(-E_A/k_BT\right)$, where $s$ is the separation between the nodes and $\beta$ is the tunneling decay constant for alkanes from literature, $0.72\ \text{Å}^{-1}$.[5] Thus each hop through the grid depended on the proximity of the nearest neighbor nodes. The directionality of the bias voltage was defined using the unit vectors **p** (in the direction of current, from source to drain) and **h** (the direction of hopping, from the occupied node to the neighbor node) as depicted in the schematic S1.

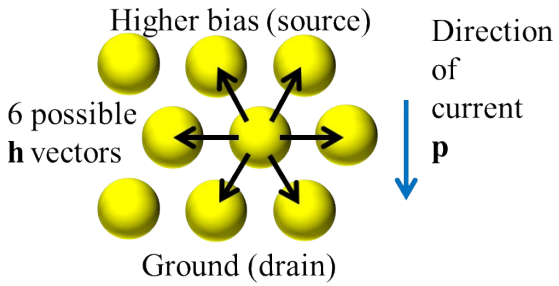


**Schematic S1. Influence of hopping direction and bias on hopping probability.** 6 **h** vectors indicate the direction of possible hops, and unit vector **p** indicates the direction from source to drain.

This method allows $V_{bias}$ to decrease the likelihood of "backwards" hops towards the source electrode and increase the likelihood of "forward" hops towards the drain electrode. A resulting $exp(0)$ in the case of horizontal hops (parallel to the length of the source and drain electrodes) means the bias does not influence sideways hops. A constant $V_{bias}$ value of 0.3464 (unitless) was used during all the simulations. The activation energy $E_A$ for alkanethiols was taken from our earlier experiments,[6] and $k_B$ and T refer to the Boltzmann constant and temperature, respectively. If a hop completes successfully, the charge moves to the new node and both successful and total number of hops increment by one. If the hop

is unsuccessful, total hops increments by one and number of successful hops remains constant. This procedure is repeated until the charge carrier reaches one of the nodes contacting the drain electrode.

PTCDI-exchanged arrays were generated according to the same protocol as the alkane arrays, except that for node separations within the acceptable range of PTCDI binding (1.7 to 2.5 nm), the tunneling term in the probability of successful hopping was increased to the single molecule conductance for PTCDI from literature.[2] The hopping probability of junctions with separations outside of this range was unaltered from the alkane case. For each grid, the calculated conductance "G" was determined by the ratio of the number of successful hops to the total number of hop attempts, $G = {N_{successful}}/{N_{total}}$. To generate sufficient statistics, 256 grids were generated for each of the 10 molecular states. The conductance ratio ($G_{ratio}$) for $C_{12}$ was the average G of the PTCDI-exchanged $C_{12}$ arrays divided by the average G of the $C_{12}$ alkane arrays, and the same method was used to calculate the $G_{Ratio}$ for $C_{14}$, $C_{16}$, $C_{18}$, and $C_{20}$.

Activation energy for alkanethiol-capped NP arrays is 17 meV.[6] Activation energy for PTCDI-state NP arrays was measured to be 26.6 ± 0.7 meV as shown in SI Section 5. The difference in the exponential term for the two activation energies is on the order of 1, while the difference in the tunneling exponentials is up to three orders of magnitude. Results for the simulations holding activation energy constant at 17 meV are below (Constant $E_A$), compared with results where alkanethiols had $E_A$=17 meV and PTCDI had $E_A$=26.6 meV (Varying $E_A$). Accounting for activation energy brings simulation results closer to experimental results but does not significantly change the trend.

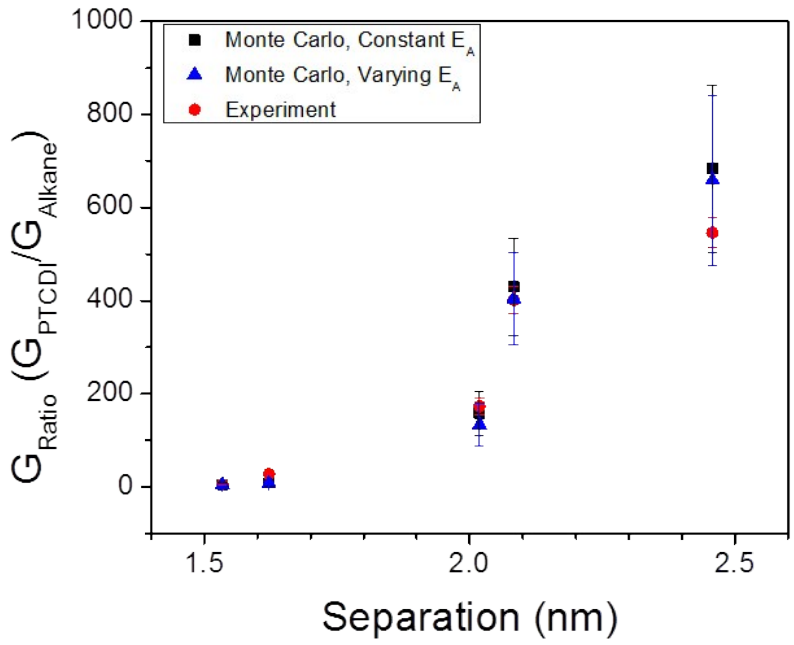


**Figure S2. Monte Carlo results with constant and varying activation energy.** Monte Carlo with constant $E_A$ uses $E_A$=17 meV for both alkane and PTCDI states. Monte Carlo with varying $E_A$ uses

$E_A$=26.6 meV for PTCDI states and 17 meV for alkane states. Using the measured $E_A$ for PTCDI brings Monte Carlo results closer to experimental results but does not significantly change the trend.

7. Method of determining ligand exchange efficiency

The size of the initial alkanedithiol and the length of the second molecule to be introduced into the nanoparticle array are both important variables in determining the ligand exchange efficiency. Using the method presented, the predicted ligand exchange efficiency can be calculated for any combination of molecules and particle separations, assuming the following variables are known.

$s_{mol2}$=secondary ligand length

μ=mean of the interparticle separation in the NP array

σ=standard deviation of interparticle separations (not to be confused with conductivity)

To find the percentage of interlinked nanoparticles, integrate over the distribution of interparticle separations within the range of acceptable molecular lengths. First the minimum and maximum molecule exchange lengths are defined:

$L_{min}$=cos(π/4)*$s_{mol2}$

$L_{max}$=$s_{mol2}$+2 Å  (here 2 Å is used for the estimated distance of an Au adatom.)

The distribution of interparticle separations are defined using a normal distribution

$$SDF = \frac{1}{\sqrt{2\pi\sigma^2}} exp\left(-\frac{(x-\mu)^2}{2\sigma^2}\right)$$

Then integrate the distribution from the minimum to the maximum acceptable lengths to find the exchange efficiency (*eff.*).

$$eff. = \int_{L_{min}}^{L_{max}} SDF \cdot dx$$

Theoretically this method is simple and versatile enough to be used with any nanoparticle array ligand exchange system for which the necessary variables are known.

References


(1) Tsutsui, G.; Huang, S.; Sakaue, H.; Sshingubara, S.; Takahagi, T. Well-Size-Controlled Colloidal Gold Nanoparticles Dispersed in Organic Solvents. *Jpn. J. Appl. Phys.* **2001**, *40* (1), 346–349.

(2) Hosseini, S.; Madden, C.; Hihath, J.; Guo, S.; Zang, L.; Li, Z. Single-Molecule Charge Transport and Electrochemical Gating in Redox-Active Perylene Diimide Junctions. *J. Phys. Chem. C* **2016**, *120* (39), 22646–22654.

(3) Schneider, C. a; Rasband, W. S.; Eliceiri, K. W. NIH Image to ImageJ: 25 Years of Image Analysis. *Nat. Methods* **2012**, *9* (7), 671–675.

(4) Advanced Chemistry Development Inc. Chemsketch, Version 12.01.

(5) Rascón-Ramos, H.; Artés, J. M.; Li, Y.; Hihath, J. Binding Configurations and Intramolecular Strain in Single-Molecule Devices. *Nat. Mater.* **2015**, *14* (5), 517–522.

(6) McCold, C. E.; Fu, Q.; Howe, J. Y.; Hihath, J. Conductance Based Characterization of Structure and Hopping Site Density in 2D Molecule-Nanoparticle Arrays. *Nanoscale* **2015**, *7* (36), 14937–14945.